

The study of calibration process for the hybrid pixel array detector of HEPS-BPIX



Ye Ding^{1,3}, Zhenjie Li¹, Wei Wei^{1,2}, Jie Zhang^{1,2}, Hangxu Li¹, Yan Zhang¹, Xiaolu Ji^{1,2}, Peng Liu¹, Yuanbai Chen^{1,2}, Kejun Zhu^{1,2}

1. Institute of High Energy Physics, Chinese Academy of Sciences, 19 B Yuquan Rd, Shijingshan District, Beijing, China.

2. State Key Laboratory of Particle Detection and Electronics, Institute of High Energy Physics, Chinese Academy of Sciences (CAS), Beijing China 100049.

3. University of Chinese Academy of Sciences (UCAS), Beijing China 100049.

dingy@ihep.ac.cn, lizj@ihep.ac.cn.

1. INTRODUCTION

HEPS-BPIX is a hybrid silicon pixel array detector which works on single photon counting mode and bases on BPIX readout chip. It consists of 16 silicon pixel modules.

□ Silicon pixel module

Table 1. The main performance of a silicon pixel module

Pixel amount	Energy range	Effective area	Pixel size
208 x 288	8 - 20 keV	3 cm x 4 cm	150 um x 150 um

As shown in Fig.1, the silicon pixel module in the HEPS-BPIX is composed of silicon sensor, readout chips and a printed circuit board (PCB).

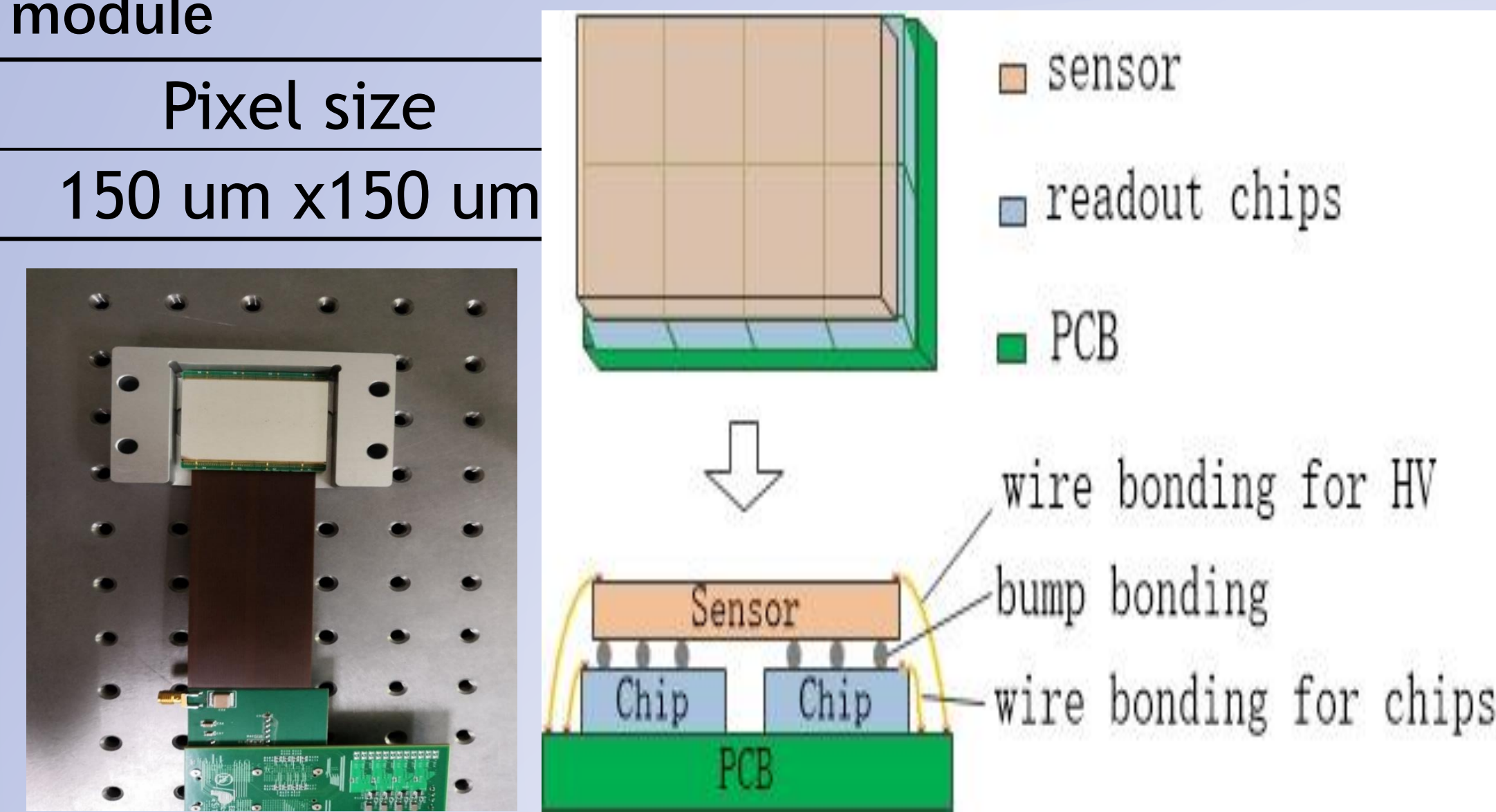


Fig. 1 The structure of a hybrid silicon pixel module.

□ Readout chip

There are 2 x 4 readout chips with 59904 cells for a silicon pixel module. The independent signal process cell of each pixel is shown in Fig. 2. The analog part includes charge sensitive amplifier (CSA), an AC coupled amplifier, discriminator. The pulse signals can be injected into the CSA to simulate the charge pulses generated in the sensor. The threshold of a pixel is adjusted by an 8-bit global DAC (GDAC) of all pixels and its own 5-bit local DAC (LDAC).

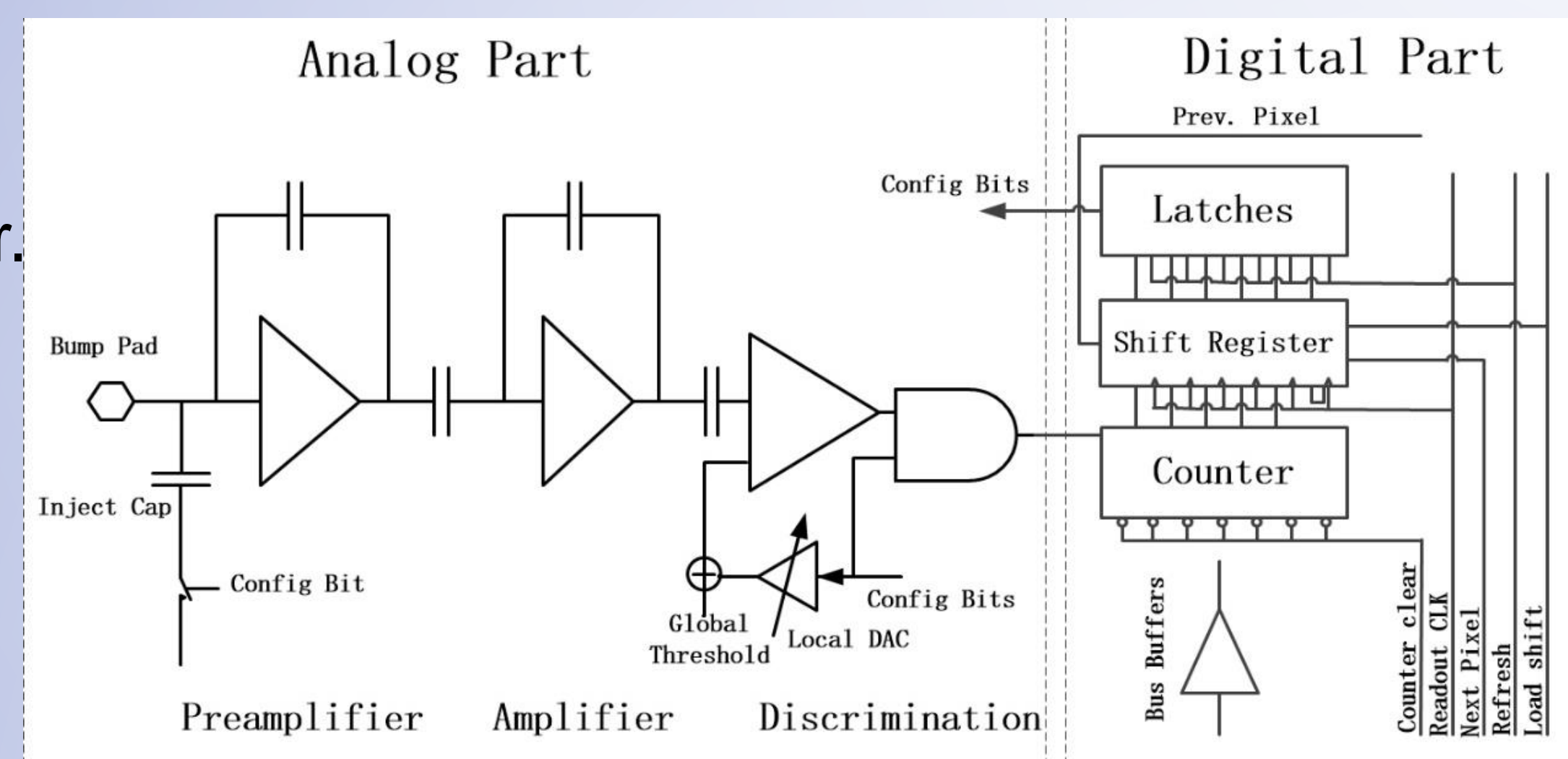


Fig. 2 The pixel signal process cell. Each pixel signal process cell of the readout chip consists of the analog part and the digital part.

2. CALIBRATION

The calibration of the silicon pixel module includes the threshold calibration and the trimming of threshold dispersion. And the test method is the threshold scanning.

□ Threshold scanning

As shown in Fig.3, the threshold scanning with noise can be described by the formula (1). The maximum noise count rate is at $V_{TH} = V_{offset}$. The equivalent noise threshold at zero count is used to quantify the maximum noise.

$$f_{noise}(V_{TH}) = f_0 \exp\left(\frac{-(V_{TH} - V_{offset})^2}{\sigma_n^2}\right) \quad (1)$$

Threshold scanning with input includes two parts: noise and input pulse. According to the S-curve method, the threshold for the input pulse is the 50% of the full count.

□ Threshold calibration

The relationship of the energy and threshold is quantified and shown in Fig.4 and formula (2). The global threshold can be set with this relationship.

$$V_{TH} = 8 * E - 26.54 \quad (2)$$

The average of the equivalent noise threshold is 17.19 GDAC LSB. Therefore, the minimum detection energy is about 5.21 ± 1.76 keV.

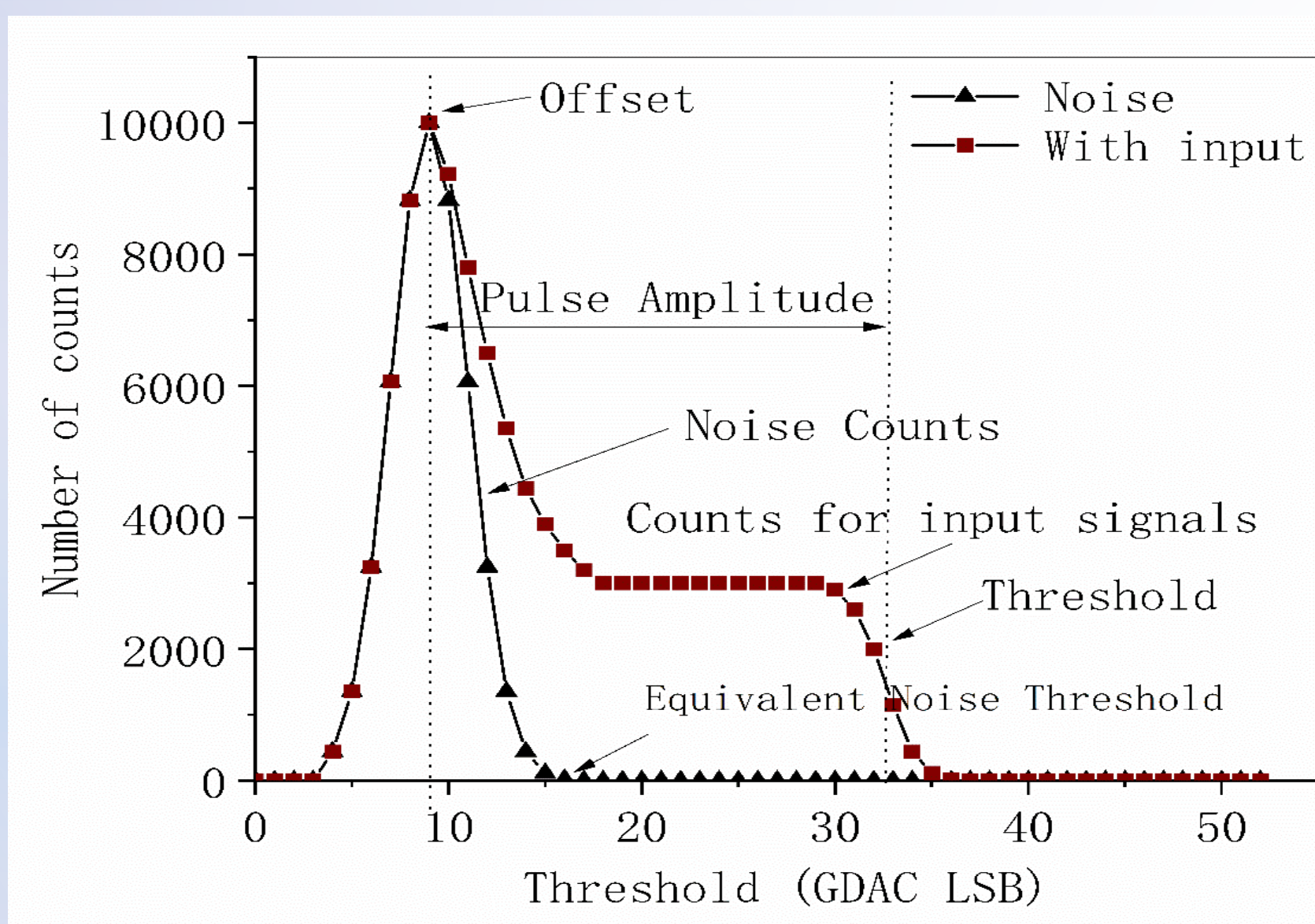


Fig. 3 Threshold scanning with noise and input pulse signals.

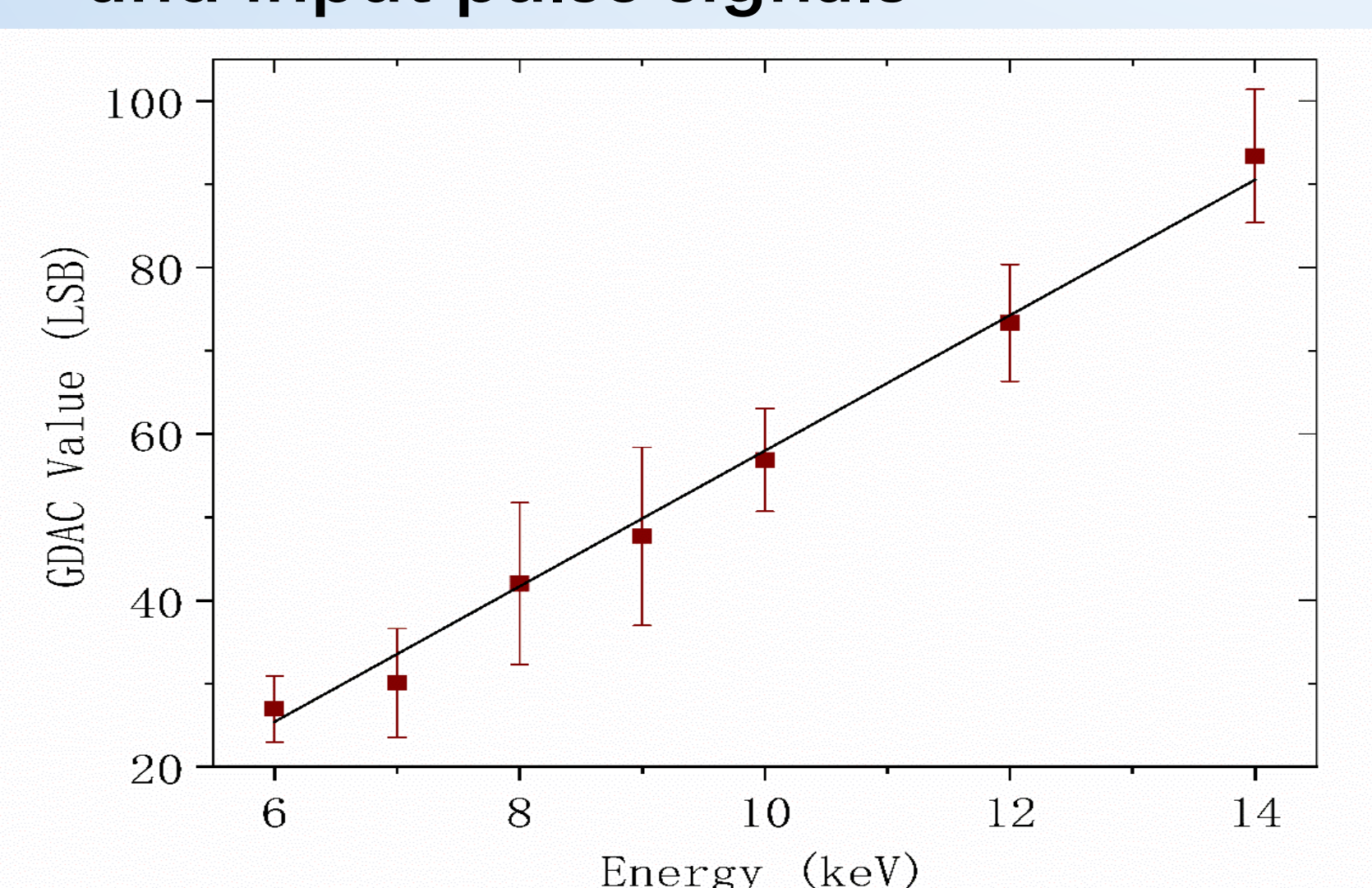


Fig. 4 The relationship of the energy and threshold.

□ Threshold Trimming

● Precise algorithm

(1) Fixed a GDAC, 32 S-curves of each pixel can be obtained by scanning the amplitudes of the input signals with each LDAC.

(2) Based on the S-curves, the character curve of each pixel can be obtained. 32 LDAC values are responding to 32 different amplitudes of input signals.

(3) Averaging the responding amplitudes of all pixels, the LDAC, where the responding amplitude is closest to the average is the proper LDAC to minimize the threshold dispersion.

● Fast algorithm

(1) Fixed the GDAC, scanning the LDAC with noise can get the equivalent noise threshold of each pixel.

(2) Fixed the input amplitude and GDAC corresponding to an energy, scanning the LDAC from 1 to 32 can get a s-curve of each pixel.

(3) To find the proper LDAC according to the S-curve and set the LDAC above the equivalent noise threshold.

The result of the threshold is presented in section 3. The fast algorithm could get the applicable threshold distribution for a silicon pixel module and take a shorter time, while the precise algorithm could get better threshold distribution, but time consuming.

□ Temperature dependence

The parameters of the chips such as threshold voltage, mobility, the intrinsic carrier concentration of silicon, etc, vary to the temperature. The temperature dependence of the noise and threshold trimming is tested. And the results are shown in section 3.

3. RESULTS

The results of threshold trimming with the precise and fast algorithm are shown in Table.2 and Fig.6.

As shown in Fig. 7, the equivalent noise threshold of the silicon pixel module increases with the temperature. The temperature dependence with calibrated LDAC is shown in Fig. 8.

	Equivalent Noise Charge (ENC)		Threshold	
	Mean/e-	δ/e	Mean/mV	δ/mV
before calibration	171.34	22.348	209.84	46.280
precise algorithm	162.25	18.030	263.56	6.783
fast algorithm	162.21	49.170	266.12	7.605

The imaging results of the LaB6 sample's power diffraction ring at 12keV X-ray are shown in Fig. 9. The four Bragg diffraction angles of the LaB6 sample are 0.26rad, 0.36rad, 0.44rad, and 0.51rad.

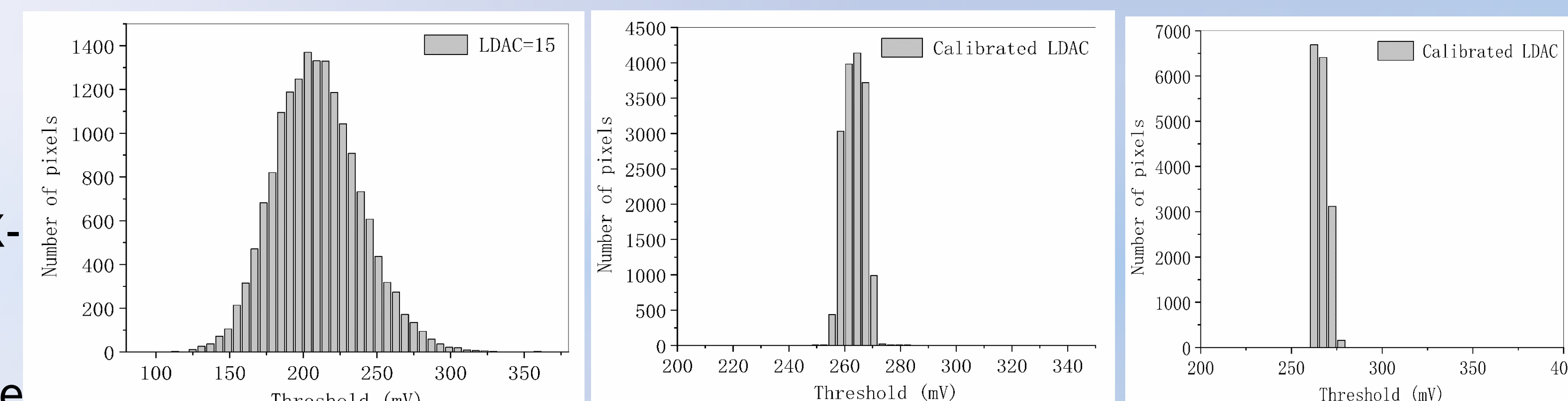


Fig. 5 The threshold dispersion before calibration.

(a) Precise algorithm. (b) Fast algorithm. Fig. 6 The threshold dispersion with calibrated LDAC

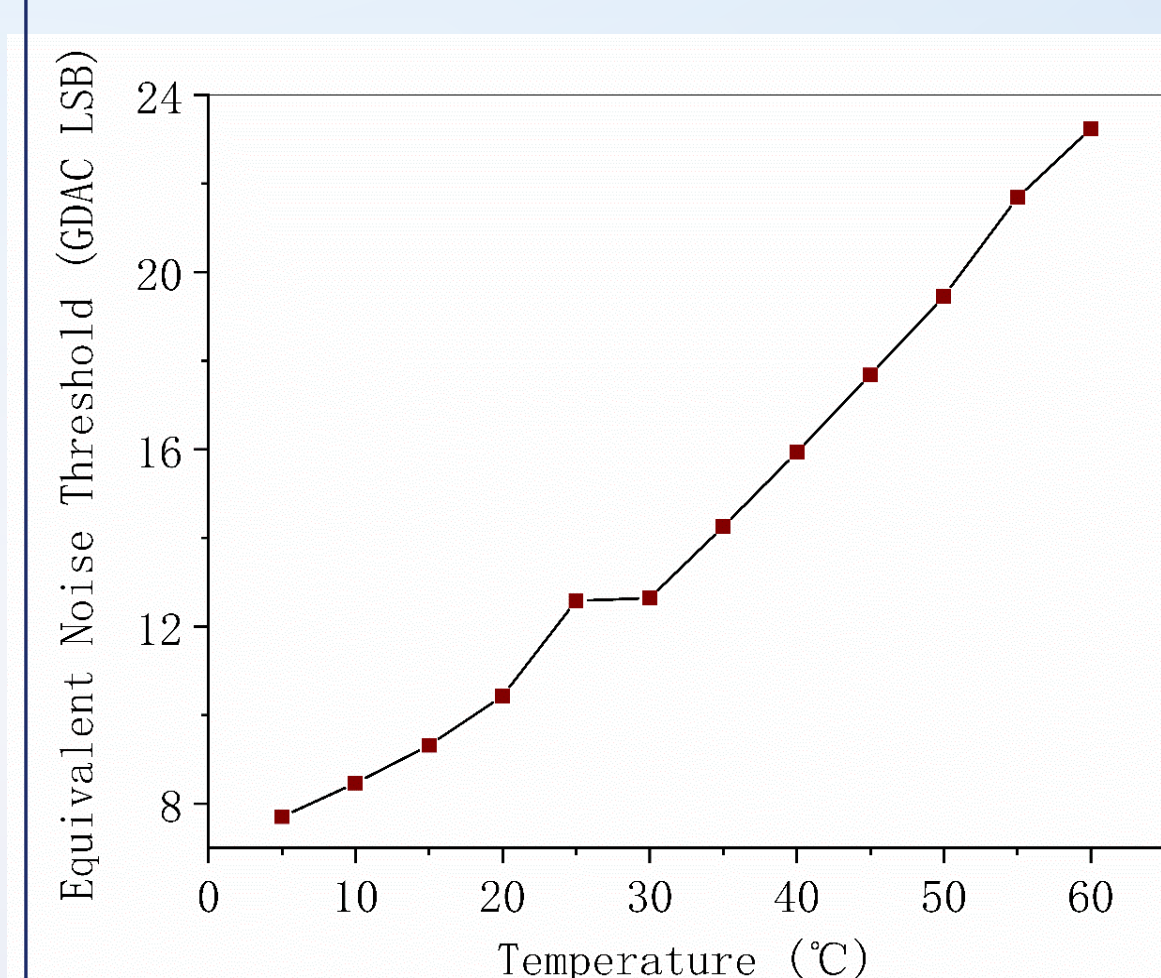
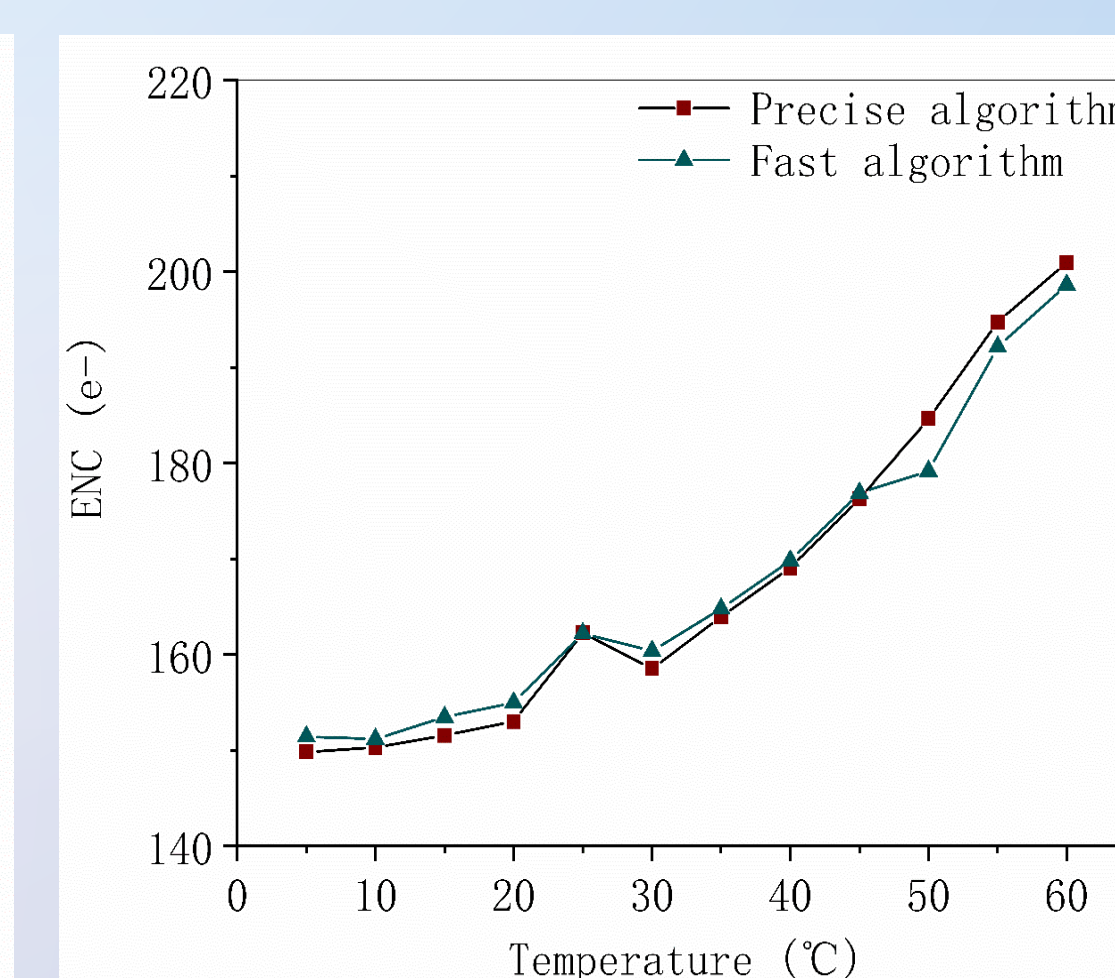


Fig. 7 The equivalent noise threshold vs temperature.



(a) ENC.

Fig. 8 The temperature dependence with calibrated LDAC.

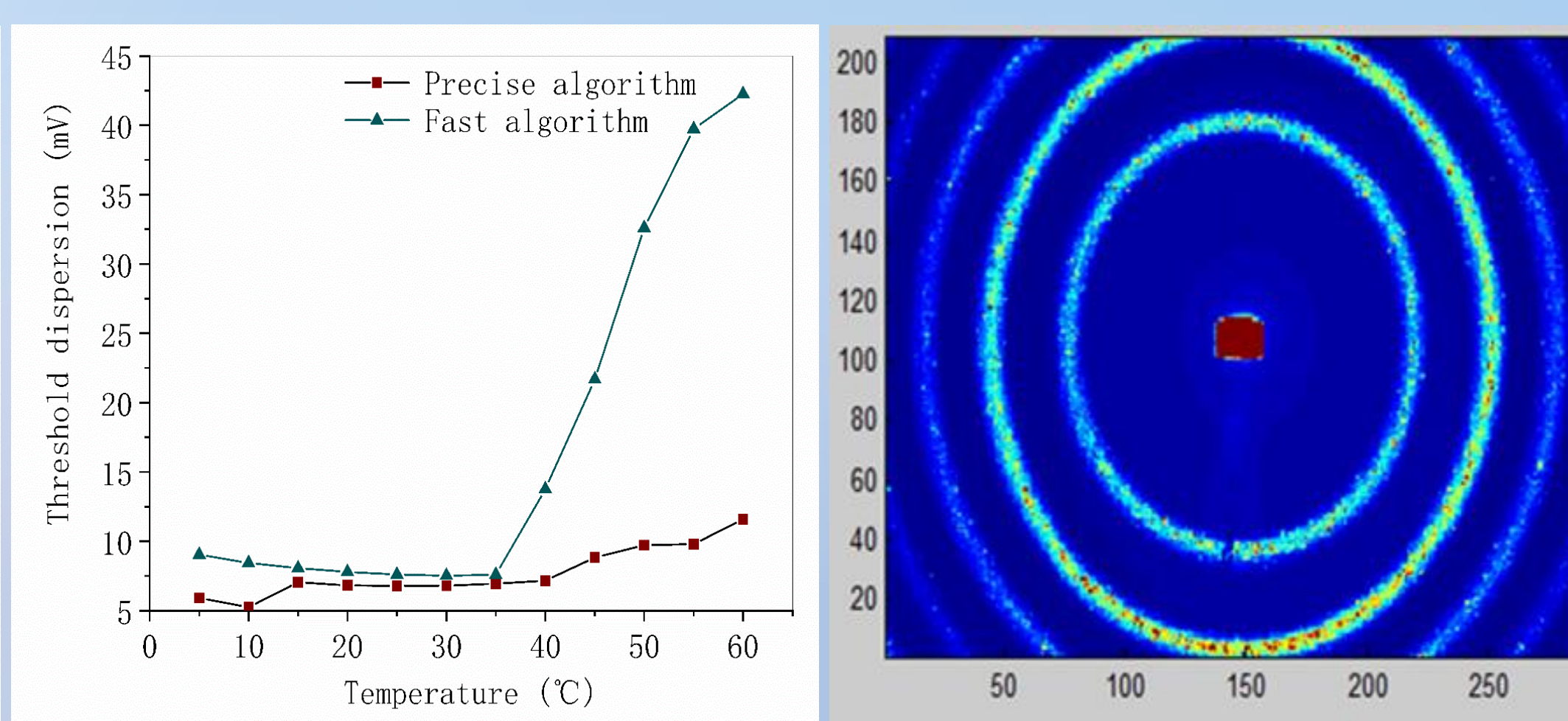


Fig. 9 The image of the X-ray diffraction.

ACKNOWLEDGMENT

The authors acknowledge the IHEP for providing funding and fundamental resources for experiments. All opinions and views in this poster are solely the responsibility of the first author and do not necessarily represent IHEP and other authors.